AFRL-RX-WP-JA-2017-0369

HIGHLY CONCENTRATED SEED-MEDIATED SYNTHESIS OF MONODISPERSED GOLD NANORODS (POSTPRINT)

Kyoungweon Park, Ming-siao Hsiao, Yoon-Jae Yi, Sarah Izor, and Ali Jawaid

UES

Richard A. Vaia and Hilmar Koerner

AFRL/RX

14 Jun 2017
Interim Report

AIR FORCE RESEARCH LABORATORY
MATERIALS AND MANUFACTURING DIRECTORATE
WRIGHT-PATTERSON AIR FORCE BASE, OH 45433-7750
AIR FORCE MATERIEL COMMAND
UNITED STATES AIR FORCE

REPORT DOCUMENTATION PAGE

Form Approved
OMB No. 0704-0188

1. REPORT DATE *(DD-MM-YY)*	2. REPORT TYPE	3. DATES COVERED *(From - To)*
14 June 2017	Interim	30 March 2015 – 14 May 2017

4. TITLE AND SUBTITLE
HIGHLY CONCENTRATED SEED-MEDIATED SYNTHESIS OF MONODISPERSED GOLD NANORODS (POSTPRINT)

5a. CONTRACT NUMBER
FA8650-11-D-5801-0014

5b. GRANT NUMBER

5c. PROGRAM ELEMENT NUMBER
61102F

6. AUTHOR(S)
1) Kyoungweon Park, Ming-siao Hsiao, Yoon-Jae Yi, Sarah Izor, and Ali Jawaid – UES
2) Richard A. Vaia - AFRL/RX

5d. PROJECT NUMBER
3002

5e. TASK NUMBER 0014

5f. WORK UNIT NUMBER
X10D

7. PERFORMING ORGANIZATION NAME(S) AND ADDRESS(ES)
1) National Research Council
500 5th St NW Ste 1
Washington, D.C. 20001
2) AFRL/RX
Wright-Patterson AFB, OH 45433

8. PERFORMING ORGANIZATION REPORT NUMBER

9. SPONSORING/MONITORING AGENCY NAME(S) AND ADDRESS(ES)
Air Force Research Laboratory
Materials and Manufacturing Directorate
Wright-Patterson Air Force Base, OH 45433-7750
Air Force Materiel Command
United States Air Force

10. SPONSORING/MONITORING AGENCY ACRONYM(S)
AFRL/RXAS

11. SPONSORING/MONITORING AGENCY REPORT NUMBER(S)
AFRL-RX-WP-JA-2017-0369

12. DISTRIBUTION/AVAILABILITY STATEMENT
Distribution Statement A. Approved for public release: distribution unlimited.

13. SUPPLEMENTARY NOTES
PA Case Number: 88ABW-2016-2932; Clearance Date: 14 Jun 2016. This document contains color. Journal article published in Applied Materials & Interfaces, Vol. 9, No. 31, 9 Aug 2017.
The final publication is available at www.acsami.org DOI: 10.1021/acsami.7b08003

14. ABSTRACT ***(Maximum 200 words)***

The extremely large optical extinction coefficient of gold nanorods (Au- NRs) enables their use in a diverse array of technologies, ranging from plasmonic imaging, therapeutics and sensors, to large area coatings, filters, and optical attenuators. Development of the latter technologies has been hindered by the lack of cost-effective, large volume production. This is due in part to the low reactant concentration required for symmetry breaking in conventional seed-mediated synthesis. Direct scale up of laboratory procedures has limited viability because of excessive solvent volume, exhaustive postsynthesis purification processes, and the generation of large amounts of waste (e.g., hexadecyltrimethylammonium bromide(CTAB)). Following recent insights into the growth mechanism of Au-NRs and the role of seed development, we modify the classic seed-mediated synthesis via temporal control of seed and reactant concentration to demonstrate production of Au-NRs at more than 100-times the conventional concentration, while maintaining independent control and narrow distribution of nanoparticle dimensions, aspect ratio, and volume. Thus, gram scale synthesis of Au-NRs with prescribed aspect ratio and volume is feasible in a 100 mL reactor with 1/100th of organic waste relative to conventional approaches.

15. SUBJECT TERMS
gold nanorods; growth mechanism; scale-up synthesis; seed-mediated growth; small-angle X-ray

16. SECURITY CLASSIFICATION OF:			17. LIMITATION OF ABSTRACT:	18. NUMBER OF PAGES	19a. NAME OF RESPONSIBLE PERSON (Monitor)
a. REPORT	b. ABSTRACT	c. THIS PAGE			Richard Vaia
Unclassified	Unclassified	Unclassified	SAR	11	19b. TELEPHONE NUMBER *(Include Area Code)* (937) 255-9209

ACS APPLIED MATERIALS & INTERFACES

Research Article

www.acsami.org

Highly Concentrated Seed-Mediated Synthesis of Monodispersed Gold Nanorods

Kyoungweon Park,[†,‡] Ming-siao Hsiao,[†,‡] Yoon-Jae Yi,[†,‡] Sarah Izor,[†,‡] Hilmar Koerner,[†] Ali Jawaid,[†,‡] and Richard A. Vaia*[,†]

[†]Materials and Manufacturing Directorate, Air Force Research Laboratory, Wright-Patterson AFB, Ohio 45433-7702, United States

[‡]UES, Inc., Dayton, Ohio 45432, United States

Supporting Information

ABSTRACT: The extremely large optical extinction coefficient of gold nanorods (Au-NRs) enables their use in a diverse array of technologies, rnging from plasmonic imaging, therapeutics and sensors, to large area coatings, filters, and optical attenuators. Development of the latter technologies has been hindered by the lack of cost-effective, large volume production. This is due in part to the low reactant concentration required for symmetry breaking in conventional seed-mediated synthesis. Direct scale up of laboratory procedures has limited viability because of excessive solvent volume, exhaustive postsynthesis purification processes, and the generation of large amounts of waste (e.g., hexadecyltrimethylammonium bromide(CTAB)). Following recent insights into the growth mechanism of Au-NRs and the role of seed development, we modify the classic seed-mediated synthesis via temporal control of seed and reactant concentration to demonstrate production of Au-NRs at more than 100-times the conventional concentration, while maintaining independent control and narrow distribution of nanoparticle dimensions, aspect ratio, and volume. Thus, gram scale synthesis of Au-NRs with prescribed aspect ratio and volume is feasible in a 100 mL reactor with 1/100th of organic waste relative to conventional approaches. Such scale-up techniques are crucial to cost-effectively meet the increased demand for large quantities of Au-NRs in emerging applications.

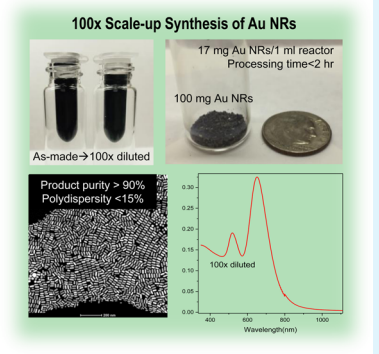

KEYWORDS: *scale-up synthesis, gold nanorods, small-angle X-ray, growth mechanism, seed-mediated growth*

INTRODUCTION

Colloidal gold nanorods (Au-NRs) have been at the center of plasmonic nanoparticle research for decades because of a direct correlation between their localized surface plasmon resonances, geometry, and composition.[1−3] Today, numerous laboratory methods provide control of size, shape, composition, crystallinity, and facet orientation.[4−9] For example, Ag-assisted, seed-mediated methods[10,11] are extensively used for high-quality, single-crystalline Au-NRs.[10−14] These initial methods have been further refined by expanding the types of additives in the growth solution, and modifying the reaction environment.[9] Seedless approaches have also been introduced, where a very low concentration of aqueous $NaBH_4$ solution is directly added to the growth solution to drive homogeneous nucleation.[15] Various recent reports focus on optimizing the seedless approach to address issues, such as polydispersity, byproducts and limited tunability of volume and aspect ratio of NRs by changing the type of reducing agent used in growth solution or adding various additives.[16,17] However, in typical seeded or seedless synthesis, Au-precursor concentration is low ($[HAuCl_4] \approx 0.0005M$);[11] thus producing at the maximum ∼1 mg Au NR per 10 mL reaction solution. Additionally, surfactant concentrations of ∼0.1 M are generally required, leading to large reagent to product ratios (e.g., 364 mg CTAB/1 mg Au-NRs). Such low production rate and intense resource requirements challenges the utilization of Au-NRs in a diverse array of technologies, ranging from therapeutics, imaging and sensors, to large area coatings, filters and optical attenuators.

In general, successful transition of these small-scale laboratory procedures to large-scale production must satisfy four factors. First is *conversion yield*, reflecting the fraction of Au-salt precursor converted to Au NR product. This includes both the effectiveness of the reduction of Au salt precursor to Au[0] (reduction yield), as well as the overall ratio of Au NR product to other undesired, nanoparticle impurities (product purity). Second is *resource efficiency*, measured by the quantity of Au-NRs produced per reagent volume, time, and energy, which includes any requisite postprocessing, such as purification and separation. Third is *product quality*, quantified by the breadth of the distributions of geometric parameters. Narrow distributions reflect the method's ability to produce near monodisperse product in a form amenable to subsequent use. And fourth is *process generality*, quantified by the range of size, shape, and volume achievable through systematic

Received: June 6, 2017
Accepted: July 17, 2017
Published: July 17, 2017

DOI: 10.1021/acsami.7b08003
ACS Appl. Mater. Interfaces 2017, 9, 26363−26371

modifications of the protocols while maintaining conversion yield, resource efficiency and product quality. All four metrics must be high for cost-effective manufacturability.

Scalability of initial seed-mediated methods required improvements to conversion yield (both reduction yield and product purity) and resource efficiency, while maintaining product quality and process generality inherent to the small-scale laboratory protocols. Reduction yield was generally low (30−70% Au precursors to Au-NRs) because substoichiometric additions of reductant (ascorbic acid) was required to ensure kinetically controlled growth of the spherocylinder shape.[18] Increasing ascorbic acid to near stoichiometric concentration resulted in dumbbell shaped rods and increased byproducts.[19] This challenge was addressed via the use of weaker reducing agents such as hydroquinone and dopamine,[20,21] or gradual addition of ascorbic acid;[22] effectively increasing reduction yield to ∼100% without disrupting product purity and quality. In concert approaches to increase production include increased batch reactor volume[21] or continuous processes.[23] For example, Lohes et al. developed an automated procedure using millifluidic reactor to run three separate 3.30 L fractions to obtain ∼10.0 L solution containing approximately 1g of Au NR. Such direct volume scaling increases throughput, but does not improve resource efficiency. The larger reagent volume is accompanied by additional labor in post processing, liquid handling, and environmental issues associated with organic surfactant waste.[24] Reducing reagent volume within established protocols by direct scaling of seed and reactant concentration unfortunately alters reduction and adsorption kinetics, which has a deleterious effect on product purity and quality.[25] Seedless approaches do provide routes to concentrated Au-NRs from concentrated reactants;[15] however, the gain in *resource efficiency* is at the expense of process generality, product quality, and product purity.

Recent reports on seed development[26,27] and mechanistic processes during Au NR growth[25,28] provide additional insights to address the scalability issue. Here in, we discuss the impact of various scale-up concepts on the various growth stages. By separating growth into two sequential steps, optimized conditions for symmetry breaking at high seed concentration can be combined with optimal conditions for increasing particle volume. Using this method, we demonstrate procedures that simultaneously satisfy the four scalability factors and provide over 100-fold increase of rod production as compared to conventional seed-mediated procedures with no loss to quality or geometric tunability.

RESULTS AND DISCUSSION

A simple way to increase *resource efficiency* is to simultaneously increase both seed and reactant concentration in order to produce a larger quantity of Au-NRs in a smaller reaction volume. This will reduce reagent waste as well as post processing cost, especially those attached to handling large liquid volumes. However, *product purity* and *product quality* may suffer due to the correlation between reaction kinetics and reactant concentration. To investigate the limit of this approach, a wide range of scale up factor for either seed concentration or reactant concentration was applied and the resulting products were carefully examined. Experimental details are shown in supplementary and summarized in Table S.1. Figure 1 and Table S.2 summarize the properties of resulting Au-NRs. Here, the concentration of seeds and reactants are concurrently increased relative to standard seed-mediated conditions.[25] Specifically, the number of seeds in the growth solution is varied by changing the volume ratio of seed solution to growth solution. Note that the conditions to prepare, and the concentration of the seed solution is held constant, utilizing recent reports on optimized seed production.[29] The volume of seed solution was increased from 10 μL to 5 mL per 10 mL reaction volume, corresponding to a seed concentration scale up factor from 1 to 500 (referred as 1S to 500S hereinafter). The $HAuCl_4$ reactant concentration was

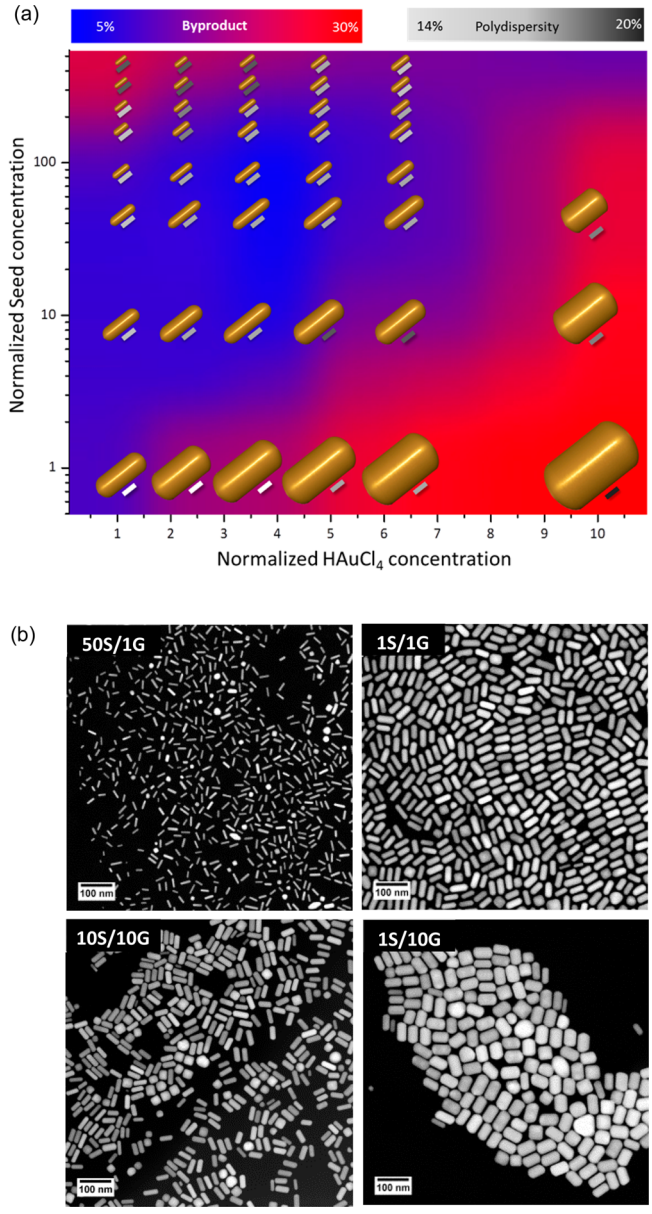

Figure 1. Impact of increasing seed concentration and reactant concentration on the structural characteristics of the Au NR product. The volume of seed solution is varied from 1S to 500S and reactant concentration was increased from 1G to 10G, where 1S and 1G are the concentration used in conventional seed-mediated protocols. (a) The change of *product quality* (polydispersity of aspect ratio) and *product purity* of resulting Au-NRs as a function of [seed] and [reactant]. The relative comparison between average dimensions of the nanorods is true to scale. The bar next to the rod indicates the polydispersity and the background color indicates the product impurities. (b) Representative TEM images of Au-NRs obtained from different condition. The scale bar is 100 nm.

DOI: 10.1021/acsami.7b08003
ACS Appl. Mater. Interfaces 2017, 9, 26363−26371

increased up to a factor of 10 (referred as 1G to 10G hereinafter). The ratio between other reactants was fixed ([$HAuCl_4$]:[$AgNO_3$]:[ascorbic acid] = 1:0.16:1.06). Finally, the concentration of CTAB was kept at 0.1 M based on parallel experiments (Figure S.1.) that revealed CTAB concentration above 0.2 M impedes Au NR quality. This effect is likely due to an increase in viscosity which disrupts reactant diffusion.[30]

The *product purity* is defined by one minus the fraction of undesired nanoparticle impurities relative to the total amount of nanoparticles produced, where one is an ideal product purity. This was estimated from UV−vis extinction spectra by the ratio between the intensity of the L-LSPR (longitudinal) to T-LSPR (transverse) peak.[31,32] The correlation between this ratio and the measured fraction of byproduct by TEM analysis was found and empirical equation to estimate the product purity was established (see discussion in experimental and Figure S.2 and Table S.4). *Product quality* was correlated with polydispersity of the structural characteristics (aspect ratio and volume) of the Au-NRs. Polydispersity of aspect ratio was estimated from the full width half-maximum (fwhm) of the solution L-LSPR in eV. This relationship is valid when the Au NR concentration is sufficiently low that the L-LSPR of the ensemble is the superposition of the inherent L-LSPR from each Au NR in solution.[24,25] The fwhm trends were also validated by the polydispersity measured by TEM analysis and the empirical equation to estimate the polydispersity from the fwhm was established (Figure S.3 and Table S.5). Polydispersity of volume and dimensions necessitated statistical image analysis of TEM micrographs of at least 1000 particles, since the impact of these factors on the absolute magnitude of the LSPR extinctions are nontrivial.[33]

Impact of Increasing Seed Concentration. First consider the impact of increasing seed concentration on a conventional reactant concentration (e.g., ***m***S where ***m*** is scale up factor for seed concentration varying from 1 to 500) at 1G ([$HAuCl_4$] = 0.00025M)), Figure 1. Since [$HAuCl_4$] is fixed, the allocated [$HAuCl_4$] per a seed decreases as the seed concentration increases. The number of rods increases and their volume decreases (Figure.S.4a). The aspect ratio however goes through a maximum at 20S (Figure S.4b). In concert, the polydispersity of aspect ratio increases slightly at the highest seed concentrations (Figure S.4c). The fraction of byproducts does not substantially change across these conditions (Figure S.4d).

These observations are consistent with the termination of Au-NRs growth upon consumption of available [$HAuCl_4$].[25] Under mild conditions, early stages (I and II) reflect isotropic seed growth followed by a symmetry breaking and rapid anisotropic growth arising from preferential micellar adsorption and passivation of the side facets. The intermediate stage (III) is characterized by adatom migration from the end to the side of the rods, resulting in a greater effective growth rate of diameter than length, and an apparent focusing of the aspect ratio distribution. As particle volume increases during this stage, the aspect ratio and its polydisperisty decreases. For conditions with 1G or greater, late stages (IV and V) are characterized by a reduction in atom addition, slow structural changes, and the development of the thermodynamically stable crystal facets. The observation at higher seed loadings of a maximum aspect ratio and an increasing polydispersity implies that partitioning of available [$HAuCl_4$] to more seeds at 1G condition simply arrests the growth at an early point. 20S then likely corresponds to cessation of growth late in stage II. Additionally since the fraction of byproducts was not changed, growth at these higher seed concentration still confirms to mild reduction conditions where final particle morphology is determined by seed structure.[26] Similar overall observations have been reported[34] when the seed to Au(III) molar ratio was changed at 1G. Such a corollary to increasing seed concentration implies that for these conditions (1S to 500S and ≤1G), traditional mild conditions and associated mechanism apply.

Impact of Increasing Reactant Concentration. Next consider the impact of increasing reactant concentration for a conventional seed addition (e.g., ***n***G where ***n*** is scale up factor for reactant concentration varying from 1 to 10 at 1S), Figure 1. Example morphology of Au-NRs formed at these higher [$HAuCl_4$] is shown in Figure 1 b. Overall, the greater [$HAuCl_4$] resulted in increased particle volume with a decreased aspect ratio, but a higher fraction of byproduct and higher polydispersity (Figure S.5). The increased byproducts indicate that the resultant increase in reduction and growth rate hampers symmetry breaking, confirming that this step and the associated formation of CTAB bilayer on (110) facets of the seeds is the slowest and most kinetically sensitive.[28] The larger volume and lower aspect ratio are consistent with the greater concentration of [$HAuCl_4$] moving the process further into stage III as discussed above.

Impact of Simultaneous Increase of Seeds and Reactants. Finally, consider the simultaneous increase of seeds and reactants, Figure 1. For example, 10S/10G system is expected to produce 10 times more rods of the same volume as the 1S/1G reaction if mild conditions prevailed. However, as noted above, this does not hold for large reactant concentrations, where the byproduct fraction increases. UV−vis NIR spectroscopy and SAXS comparison between 1S/1G and 10S/10G (Figure.S.6) confirm these effects, such as an early onset of transversal growth producing a shorter, wider rod. Substantially more seeds (100S) are necessary to provide sufficient heterogeneous growth sites to accommodate an intermediate increase in reactant concentration (1G-3G), but at a cost of *process generality*. At the higher reactant concentrations (>5G), no adjustment of seed concentration is sufficient to retain a *product purity*.

In summary, some scale up of the conventional seed-mediated recipe without significant impact on *product purity* and *product quality* is feasible by increasing seed concentration with minor increases in gold precursor concentration. The limits of such a direct scaling methodology is likely associated with the disruption of the balance between reactant reduction and micelle absorption to very small Au nanoparticles that induces symmetry breaking at the beginning of stage II. Such a balance also determines the afffectiveness of growth additives. For example, BDAC is used to produce nanorods with aspect ratios up to 8.[11] When added outside of the 1S/1G system, however, the fraction of byproducts increases severely, and the aspect ratio is reduced (Figure S.7). Thus, the directly scaling current methods provides only minor advantages at the cost of limited *process generality*.

Scale up via Two Step Growth Approach. An alternative to such direct scaling would be to separate the growth process into two steps based on the Au NR growth mechanism−first optimizing symmetry breaking of seeds at high particle concentration, and a second that reinitiates growth of these "seed-rods" by the optimized addition of reactants and additives to obtain a targeted aspect ratio and volume. One can consider such a process as sequentially "moving up S" and "across G" in

DOI: 10.1021/acsami.7b08003
ACS Appl. Mater. Interfaces 2017, 9, 26363−26371

the reaction space in Figure 1. Via this 2-step approach, the *resource efficiency* will in increased while maintaining *product quality* and *process genarality* inherent to lab-scale seed-miediated method. This concept is compared to traditional synthesis in Scheme 1. For the 2-step approach, ***m***S seeds are

Scheme 1. Scale-up Synthesis of Au-NRs via Two-Step Growth Approach Compared with Conventional Seed-Mediated Rod Growth[a]

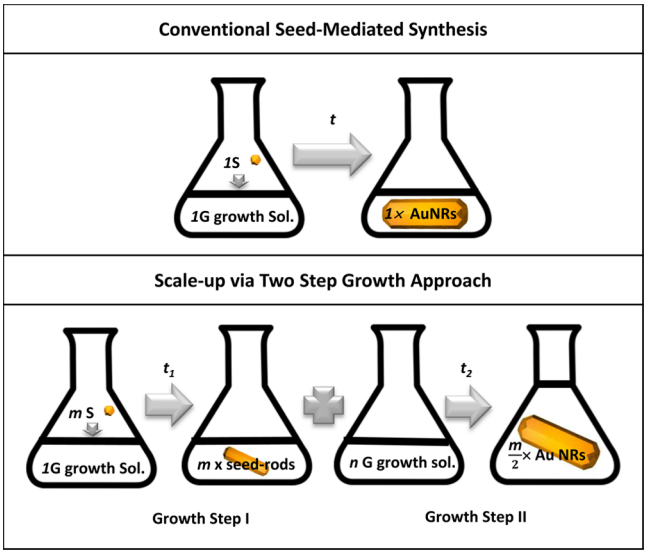

[a]Two step growth approach consist of growth step I where ***m*** times higher concentration of seeds grow in dilute growth solution(1G) for t_1 resulting ***m*** times higher concentrated seed-rods. Addition of the same volume of ***n*** times concentrated growth solution(***n***G) to the seed-rod solution initiates growth step II. This protocol can be referred as ***m***S/1G+***n***G. The final volume and concentration of the rods is determined by the factor ***m*** and ***n***.

grown in 1G growth solution for t_1, followed by the addition of the same volume of ***n***G growth solution for t_2 where ***m*** is the scale up factor of seed concentration and ***n*** is that of reactant concentration. The relative concentration of seeds and reactants for a given 2-step procedure can be denoted as ***m***S/1G+***n***G.

To illustrate this concept, Figure 2 summarizes Au NR synthesis where 20S seeds were grown in 1G growth solution, followed by the addition of the same volume of 20G growth solution (20S/1G+20G) to obtain 10 times higher concentration of Au-NRs with the same volume of rods as in 1S/1G condition (final scale-up factor of 10). Figure 2a summarizes the particle evolution kinetics of this first, "seed-rod" growth reaction (20S/1G). 20S/1G provided the highest concentration of seed-rods showing the largest aspect ratio (L-LSRP ≈ 850 nm corresponding aspect ratio of ∼4.5) during the growth. Kinetically, an L-LSPR for 20S/1G emerges at 690 nm around 2−3 min, rapidly red shifts up to 850 nm in 15 min, and then slowly blue shifts as the Au salts are depleted near the end-point of stage II. At early times (t_1 < 15 min), this is similar to 1S/1G, but at later times does not show the L-LSPR blue shift (reduced aspect ratio) associated with stage III+ growth because of the higher seed-to-reactant ratio. Here, aliquots from the initial 20S/1G seed-rod solution were removed at different points (t_1 = 1−300 min) and the same volume of second growth solution (20G) was supplied (20S/1G+20G). UV−vis-NIR spectra were taken 24 h after seed-rod addition (Figure S.7) and analyzed to estimate the characteristics of Au-NRs (Figures 2b). The aspect ratio of the final products were less than that of the seed-rods, as expected based on the reinitiation of stage III+ growth with additional reactants. Seed-rods aliquots from t_1 > 15 min produced Au-NRs of similar final aspect ratio with a relatively narrow polydisperity. The *product purity* estimated from the ratio between L-LSPR to T-LSPR showed a maximum between t_1 ≈ 15 and 30 min. Figure 2c provides representative TEM images and particle size measurement to complement and confirm the spectroscopic analysis.

This example of the 2-step growth approach indicates that the optimal time to initiate the second growth with higher reactant concentration is at the transition between stage II and III when the seed-rods have fully formed after rapid anisotropic growth. The addition of 20G solution during stage I and early stage II (t_1 < 15) significantly disturbs the initial symmetry breaking and growth of the small seed, deteriorating *product quality* and *product purity* (Figure 2b). Using longer times for the first growth step (t_1 > 30 min) also deteriorates *product quality*; the fraction of nonrod particles increases (decreasing product purity as shown in Figure 2b) and a bimodal distribution of rod length (Figure 2c) emerges. This is likely related to the transient character of the stage II rods that even in the absence of addition Au precursors, facet restructuring, adatom migration, CTAB bilayer rearrangement, etc. continue.[25,35] Overall, the highest aspect ratio, narrowest polydispersity, and least impurities for this 20S/1G+20G example occurred when seed-to-growth solution concentrations were optimized such that initial step (seed-rod growth) terminated at the end of stage II (t_1 ≈ 15 and 30 min). This implies that the growth mechanism involved in stages I and II is not perturb by higher seed concentration, consistent with the results discussed in Figure 1 and 2a. Neither the reduced CTAB concentration, nor Ag concentration, per nanorod in this first step negatively impacts the symmetry breaking process. This implies that the traditional formulation for Au NR growth (1S:1G) contains Ag and CTAB in excess of what is necessary for initial rod formation, and as discussed below, sufficient for symmetry breaking up to at least 100S.

Figure 3 summarizes the scale up feasibility of this 2-step strategy. Figure 3a shows UV−vis spectra of Au NR solutions produced at 12.5 (25S/1G+25G), 25 (50S/1G+50G), and 50 (100S/1G+100G) times the concentration of conventional 1S/1G synthesis. Note that the spectrum was taken from the reaction solution diluted via the scale up factor, and thus reflects the same particle concentration if the process was ideal. The experimental details, including aging time of the seed-rods, are shown in supplementary (Table S.2). For example, 50S seed solution was grown in 1G solution to seed-rods, then add to an equal volume of 50G (50S/1G+50G). The result is ∼50 times higher number of rods in twice the reaction volume; other words 25 times rod concentration than in the conventional 1S/1G synthesis.

The properties of resulting Au-NRs were evaluated via spectral analysis and shown in Figure 3b. The overall *product quality*, as reflected by general UV−vis spectra, is comparable as particle concentration is increased. The similar absorbance at 400 nm indicates that Au *reduction yield* was preserved.[31] The estimated Au reduction yield was 67% which can be further increased close to 100% by gradually adding ascorbic acid afterward. The equivalent shape of the T-LSPR peak and the

DOI: 10.1021/acsami.7b08003
ACS Appl. Mater. Interfaces 2017, 9, 26363−26371

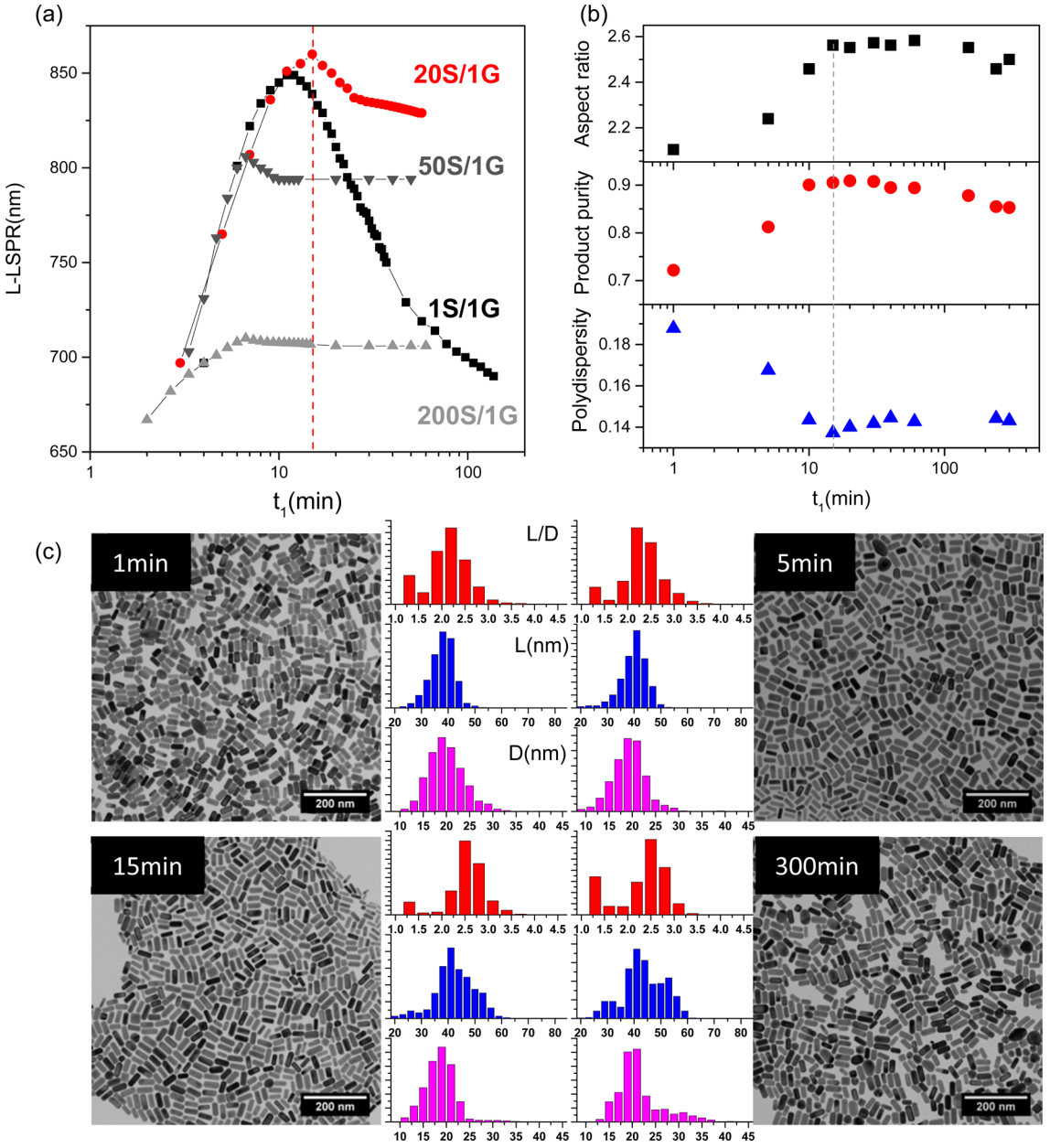

Figure 2. Synthesis of Au-NRs in 20S/1G+20G reaction condition. (a) Seed rod growth monitored via change in L-LSPR during the Au NR growth with increasing seed concentration from 1S to 200S. (b) Characteristics of Au-NRs grown from 20S/1G+20G condition. The 20G growth solution was added to the 20S/1G solution at t_1 after its preparation. (c) TEM images from the resulting particles. Size distribution of aspect ratio (L/D), length (L), and diameter (D) is shown next to each TEM image.

ratio between L-LSPR to T-LSPR suggest that the fraction of nonrod particles is similar for all conditions, indicating that *product purity* was also maintained. TEM image and size analysis summarized in Figure 3c and d confirm that there is no significant difference in dimension of the rods, verifying successful process control. Since the Au *reduction yield* was similar as the scale up factor increases and the quality of the Au-NRs is similar, *the resource efficiency* increases by analogous factors (i.e., 12.5, 25, and 50) without deteriorating *the product quality and product purity*.

The practical maximum scale up was found to be around 100 (200S/1G+200G). Figure 4 summarizes the characteristics of Au-NRs from 100× scale up. Figure 4a shows Au NR solution prepared from 200S/1G+200G condition where 1 mL reaction volume initially contains 33.9 mg $HAuCl_4$ in growth solution (corresponding Au weight is19.6 mg). The maximum Au reduction yield was obtained by postaddition of ascorbic acid and estimated as 99% by the intensity at 400 nm from the UV–vis spectrum (Figure 4a, taken from 100x diluted solution in 1 cm cuvette). The resulting product contains 10% of spherical byproducts. Therefore, the amount of Au-NRs obtained from the 100× scale up reaction is estimated to ∼17 mg per 1 mL reactor. To obtain 1g of nanorods, the reaction volume is increased to 60 mL. Here, *product quality* and *purity* become less consistent due to the highly unstable nature of the 200G growth solution. Controlling reduction with ascorbic acid at such high concentration of $HAuCl_4$ and $AgNO_3$ is difficult, often resulting unwanted nanoparticle formation. Further increases in particle concentration beyond 100× may be possible however by increasing uniformity and reducing

DOI: 10.1021/acsami.7b08003
ACS Appl. Mater. Interfaces 2017, 9, 26363−26371

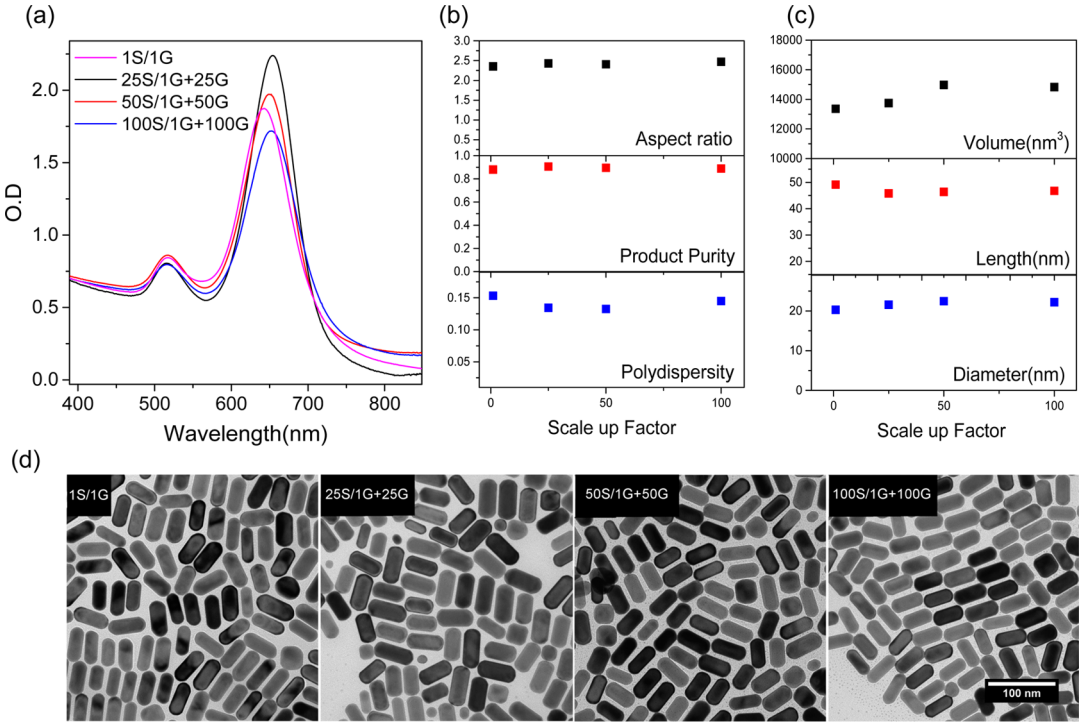

Figure 3. Growth of Au-NRs via 2-step protocol. The scale up factors of [seed] and [reactant] were increased up to 100. (a) UV−vis spectra of the resulting Au-NRs. (b) The product characteristics of resulting Au-NRs assessed via spectral analysis (c) Structural characteristics of resulting Au-NRs accessed via TEM analysis. (d) Representative TEM images of corresponding Au-NRs grown from increasing scale up factor.

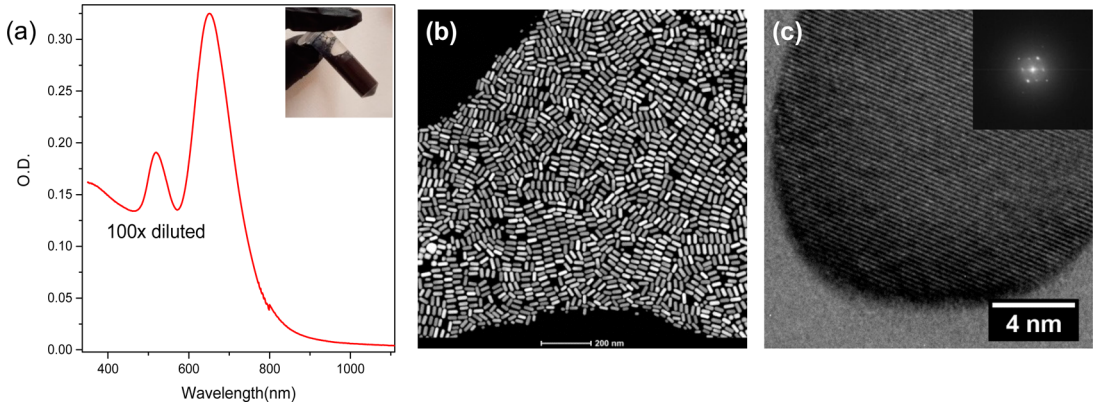

Figure 4. Characteristics of Au-NRs produced from 200S/1G+200G reaction. (a) UV−vis extinction spectrum. Inset shows the 1 mL reaction solution containing 17 mg of Au-NRs. (b) STEM image of resulting Au-NRs. (c) HR TEM image and analysis on crystalline facets. Inset shows corresponding FFT.

reduction rate via design of the reaction vessel, reagent addition processes, or use of alternatives to ascorbic acid. High-resolution TEM images (Figure 5c) also confirm that the single crystalline structures of Au-NRs from this process production is identical to that of typical synthesis.

It is noteworthy to also mention that as the scale-up factor increases, the processing time can be decreased significantly. For a typical 1S/1G condition, growth is nominally complete after 40−60 min at room temperature, as reflected by saturation of extinction intensity at 400 nm. In contrast, the growth time decreases to 20−5 min for scale up factor of 10−50, respectively. The reduced production time enhances resource efficiency further.

Tuning Volume and Aspect Ratio via Two-Step Growth Approach. Since the conditions outlined enable the separation of nanorod concentration (S) from nanorod volume (G), the 2-step growth concept also provides a direct way to control volume and aspect ratio of rods, thus retaining the hallmark of seed-mediated growth—*process generality*. Defining $1V$ as the volume of the nanorod produced from the typical one-step 1S/1G reaction, a mS/1G+nG formulation will yield nanorods of volume $\left(\frac{n}{m}\right)\cdot V$ assuming similar conversion yield. Figure 5 demonstrates this volume tunability at high reaction concentrations. Au-NRs of three different volumes were targeted by deliberately increasing the scale up factor of seed at fixed reactant concentration (10S/1G+30G, 30S/1G+30G and, 90S/1G+30G). The volume of the resulting nanorods decreases as seed concentration increases (Figure 5d) with maintaining *product quality* and *product purity* (TEM shown in Figure 5a−c). Note that tuning of the volume can be also achieved by the ratio of volume of seed-rod solution and

DOI: 10.1021/acsami.7b08003
ACS Appl. Mater. Interfaces 2017, 9, 26363−26371

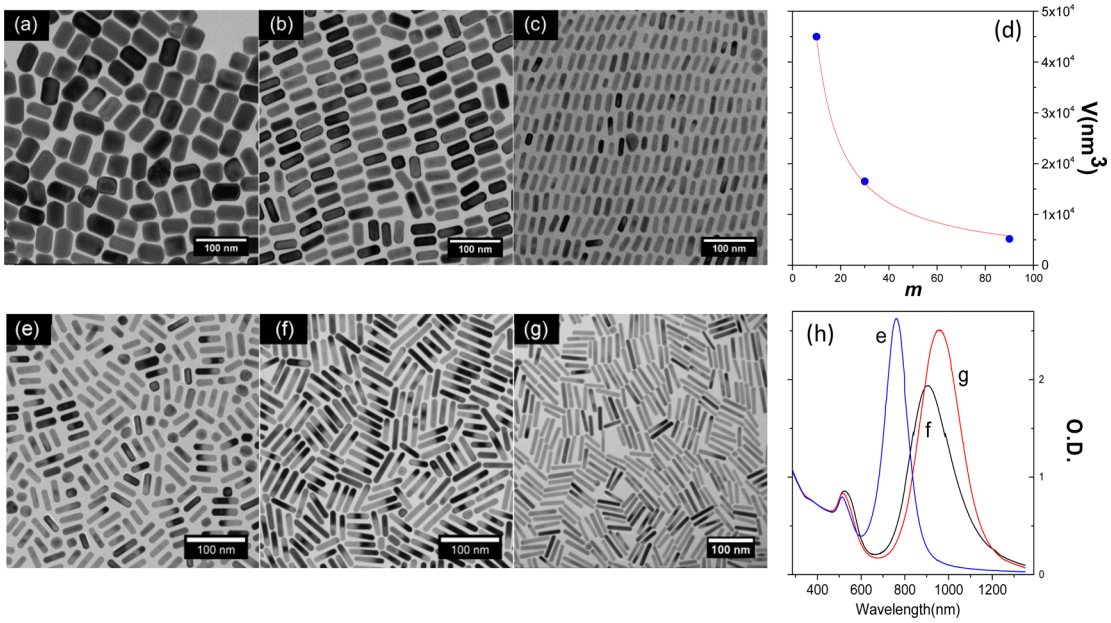

Figure 5. Tuning the volume and aspect ratio via 2-step protocol: (a–c) TEM images of different volume of NRs prepared via changing seed concentration in scale-up production (d) The correlation between seed concentration scaling factor (***m***) and volume(V) of the resulting nanorods. (e–g) TEM images of different aspect ratio of NRs prepared via changing the surfactant composition in 2nd growth solution (BDAC concentration from 0.05, 0.1, and 0.125, respectively). (h) UV–vis extinction spectra of the resulting NR solutions. All scale bars are 100 nm.

Table 1. Comparison of Efficiency of Various Scale-up Approaches to Synthesize Au-NRs

	resource efficiency (to produce 1g Au-NRs)							
			processing time		conversion yield			
	reaction volume (mL)	CTAB consumption (mg)	synthesis (h)	post processing (h)	Au reduction (%)	NR purity	product quality	product generality
Liz-Marzan[20]	5000	18500	>4	>8	~99	N/A	N/A	N/A
Kozek et al.[21]	5385	20000	>4	>8	~99	N/A	N/A	N/A
Lohes et al.[23]	10000	36200	>4	>8	N/A	N/A	N/A	N/A
Vigderman et al.[22]	5000	18500	>4	>8	~99	N/A	N/A	N/A
This study 200S/1G+200G reaction	60	218	<1	<1	~99	>0.9 similar to typical 1S/1G reaction	<15% similar to typical 1S/1G reaction	tunable volume and aspect ratio ($L/D \approx 6$)

second growth solution at fixed S and G. When reacion condition is following, V_1(mS/1G) + V_2(nG), where V_1 is the volume of seed-rod solution and V_2 is the volume of second growth solution, The volume of the rod can be estimated as $\frac{V_2 n}{V_1 m}$.

Similarly, the aspect ratio of the rods can be tuned at these high concentrations by prescibing the necessary additives in the second growth solution. For a conventional synthesis, higher aspect ratio NRs (up to ~10) require modification of growth solution, such as varying $AgNO_3$ concentration,[11] adding cosurfactants, such as benzyldimethylhexadecylammonium chloride (BDAC)[11,32] various aromatic additives,[9] or changing temperature[36] and pH.[37] For example, Figures 5e-h summarize the use of BDAC to promote the formation of denser surfactant layer on the seed-rods. Specifically, three seed-rod solutions were prepared at 100S/1G condition. At the end of stage II, a certain amount of BDAC was added to the seed-rod solution to make 0.05, 0.1, and 0.125 M BDAC concentration in solution, followed by ~10 min hold to enable equilibration. The same volume of three 100G growth solutions which also contain 0.05, 0.1, and 0.125 M BDAC was prepared and added to the corresponding seed-rod solutions. As the concentration of BDAC increased, the aspect ratio increased from 3.5, 5, and 6. As is shown in the UV–vis spectra (Figure 5h), the resulting longer nanorods maintain product quality and product purity.

Note that even with 100× scale up, the resulting NRs stay well-dispersed throughout the synthesis and subsequent storgage of the colloidal solution. Au-NRs are electrostatically stabilized in water due to the postive particle charge arising from the CTAB bilayer. The minimum CTAB concentration to form this bilayer can be estiamted from the area per CTAB molecule (~0.22 nm^2) and the size and concentration of Au-NRs. From TEM, the surface area of a typical Au NR obtained from 100× scale-up (50 nM) is ~2200 nm^2. The minumum CTAB concentration to form the bilayer is thus ~0.5 mM. This is substantially lower than the CTAB concentration in the growth solution (0.1 M), consistent with the observed colloidal stability. Such estimates of minimum CTAB concentration are utilized in postprocessing where the reactant product is pelletized and redispersed in water with a lower CTAB concentration to minimize potential deleterious impact of CTAB on surface fucntionalization, polymer blending, and bio toxicity. Furthermore, the excess CTAB present even at 100× scale-up also enables pelletaization of the rods, solid state

DOI: 10.1021/acsami.7b08003
ACS Appl. Mater. Interfaces 2017, 9, 26363–26371

storage and redisperion, as shown in the Table of Contents. A wet solid powder can be easily obtained by evaporating water. This powder (~5% w/w water) can be redispersed in water with minimal aggeregation. Note that complete removal of water, such as by vacuum drying, inhibits complete redispersion.

Finally, Table 1 compares the scale-up effectiveness of the 2-step strategy relative to other literature reports of large-scale production of Au-NRs. *Resource efficiency* is compared assuming the production of 1g of Au-NRs. The 2-step strategy requires 50 mL reaction volume while other approaches need at least 5 L. Additionally, the consumption of CTAB is dramatically decreased by 50 fold. The estimated time to complete the synthesis and the post processing is also significantly lowered. Taken together, the cost of production is expected to lower accordingly. Product quality, product purity and process generality unfortunately cannot be quantitatively compared across these approaches, since required measurements are not available in the literature.

CONCLUSION

Effective scale up of conventional lab-scale seed-meditated Au NR synthesis requires the simultaneous increase of seed and reactant concentration. However, increasing reactant concentration beyond 4−5 times significantly affects the growth kinetics and results in deterioration of product quality and product purity. An alternative approach based on separation of the initial symmetry breaking of the seed (stages I and II) from subsequent coarsening of the Au NR (stage III+) enabled scale up to 100 times. Specifically, the first step provides a concentrated solution of "seed-rods" using a high concentration of seeds (up to 200S) in a relative dilute growth solution (1G). The second step adds these "seed-rods" to a concentrated growth solution with growth modifies to produce a high concentration of final product. *Product purity* and *quality* is conserved since the symmetry breaking was not disturbed in a 1G growth solution. The *process generality* is also retained by tuning the scale up factor of seed-rod and reactant concentration, as well as the addition of cosurfactant to the second growth step. Compared to prior reports, the 2-step approach provides a 100-fold increase to *resource efficiency* relative to reaction volume and CTAB consumption. Scale up beyond 100 times is currently limited by the reproducible preparation of a stable growth solution at higher reactant concentration. This challenge could be addressed via optimization of reagent feed rate, use of alternative reductants, controlled atmosphere, and design of the reaction vessel to increase solution uniformity. In conclusion, the new 2-step scale up protocol resolves many issues associated with direct scale up of traditional laboratory methods for seed-mediated synthesis and provides an economical route to accelerate the use of Au-NRs in a diverse array of technologies, ranging from plasmonic imaging, therapeutics, and sensors, to large area coatings, filters, and optical attenuators.

ASSOCIATED CONTENT

Supporting Information

The Supporting Information is available free of charge on the ACS Publications website at DOI: 10.1021/acsami.7b08003.

Experimental details (PDF)

AUTHOR INFORMATION

ORCID

Kyoungweon Park: 0000-0001-8069-3000

Richard A. Vaia: 0000-0003-4589-3423

Notes

The authors declare no competing financial interest.

ACKNOWLEDGMENTS

The authors extend their appreciation to Dr. Alexander Hexemer and Dr. Eric Schaible for guidance, setup, and data collection at beamline 7.3.3 at Advanced Light Source/ Lawrence Berkley National Laboratory. The authors are also grateful to Dr. Andrew Gilman for the help in schematic illustration. The research was graciously supported by the Air Force Office of Scientific Research (AFOSR) and the Air Force Research Laboratory's Materials and Manufacturing Directorate

REFERENCES

(1) Biagioni, P.; Huang, J.-S.; Hecht, B. Nanoantennas for Visible and Infrared Radiation. *Rep. Prog. Phys.* **2012**, *75*, 024402.

(2) Zijlstra, P.; Chon, J. W. M.; Gu, M. Five-dimensional Optical Recording Mediated by Surface Plasmons in Gold Nanorods. *Nature* **2009**, *459*, 410−413.

(3) Zijlstra, P.; Orrit, M. Single Metal Nanoparticles: Optical Detection, Spectroscopy and Applications. *Rep. Prog. Phys.* **2011**, *74*, 106401.

(4) Park, K.; Biswas, S.; Kanel, S.; Nepal, D.; Vaia, R. A. Engineering the Optical Properties of Gold Nanorods: Independent Tuning of Surface Plasmon Energy, Extinction Coefficient, and Scattering Cross Section. *J. Phys. Chem. C* **2014**, *118*, 5918−5926.

(5) Ming, T.; Chen, H. J.; Jiang, R. B.; Li, Q.; Wang, J. F. Plasmon-Controlled Fluorescence: Beyond the Intensity Enhancement. *J. Phys. Chem. Lett.* **2012**, *3*, 191−202.

(6) Near, R. D.; Hayden, S. C.; El-Sayed, M. A. Thin to Thick, Short to Long: Spectral Properties of Gold Nanorods by Theoretical Modeling. *J. Phys. Chem. C* **2013**, *117*, 18653−18656.

(7) Nusz, G. J.; Curry, A. C.; Marinakos, S. M.; Wax, A.; Chilkoti, A. Rational Selection of Gold Nanorod Geometry for Label-Free Plasmonic Biosensors. *ACS Nano* **2009**, *3*, 795−806.

(8) Vigderman, L.; Khanal, B. P.; Zubarev, E. R. Functional Gold Nanorods: Synthesis, Self-Assembly, and Sensing Applications. *Adv. Mater.* **2012**, *24*, 4811−4841.

(9) Ye, X.; Jin, L.; Caglayan, H.; Chen, J.; Xing, G.; Zheng, C.; Doan-Nguyen, V.; Kang, Y.; Engheta, N.; Kagan, C. R.; Murray, C. B. Improved Size-Tunable Synthesis of Monodisperse Gold Nanorods through the Use of Aromatic Additives. *ACS Nano* **2012**, *6*, 2804−2817.

(10) Jana, N. R.; Gearheart, L.; Murphy, C. J. Wet Chemical Synthesis of High Aspect Ratio Cylindrical Gold Nanorods. *J. Phys. Chem. B* **2001**, *105*, 4065−4067.

(11) Nikoobakht, B.; El-Sayed, M. A. Preparation and Growth Mechanism of Gold Nanorods using Seed-Mediated Growth Method. *Chem. Mater.* **2003**, *15*, 1957−1962.

(12) Murphy, C. J.; Sau, T. K.; Gole, A. M.; Orendorff, C. J.; Gao, J.; Gou, L.; Hunyadi, S. E.; Li, T. Anisotropic Metal Nanoparticles: Synthesis, Assembly, and Optical Applications. *J. Phys. Chem. B* **2005**, *109*, 13857−13870.

(13) Nikoobakht, B.; El-Sayed, M. A. Preparation and Growth Mechanism of Gold Nanorods (NRs) Using Seed-Mediated Growth Method. *Chem. Mater.* **2003**, *15*, 1957.

(14) Gole, A.; Murphy, C. J. Seed-Mediated Synthesis of Gold Nanorods: Role of Size and Nature of the Seed. *Chem. Mater.* **2004**, *16*, 3633−3640.

(15) Jana, N. R. Gram-Scale Synthesis of Soluble, Near-Monodisperse Gold Nanorods and Other Anisotropic Nanoparticles. *Small* **2005**, *1*, 875−882.

(16) Liopo, A.; Wang, S.; Derry, P. J.; Oraevsky, A. A.; Zubarev, E. R. Seedless Synthesis of Gold Nanorods using Dopamine as a Reducing Agent. *RSC Adv.* **2015**, *5*, 91587−91593.
(17) Xu, X.; Zhao, Y.; Xue, X.; Huo, S.; Chen, F.; Zou, G.; Liang, X.-J. Seedless Synthesis of High Aspect Ratio Gold Nanorods with High Yield. *J. Mater. Chem. A* **2014**, *2*, 3528−3535.
(18) Orendorff, C. J.; Murphy, C. J. Quantitation of Metal Content in the Silver-Assisted Growth of Gold Nanorods. *J. Phys. Chem. B* **2006**, *110*, 3990−3994.
(19) Gou, L.; Murphy, C. J. Fine-Tuning the Shape of Gold Nanorods. *Chem. Mater.* **2005**, *17*, 3668−3672.
(20) Alvarez-Puebla, R. A.; Agarwal, A.; Manna, P.; Khanal, B. P.; Aldeanueva-Potel, P.; Carbo-Argibay, E.; Pazos-Perez, N.; Vigderman, L.; Zubarev, E. R.; Kotov, N. A.; Liz-Marzan, L. M. Gold Nanorods 3D-Supercrystals as Surface Enhanced Raman Scattering Spectroscopy Substrates for the Rapid Detection of Scrambled Prions. *Proc. Natl. Acad. Sci. U. S. A.* **2011**, *108*, 8157−8161.
(21) Kozek, K. A.; Kozek, K. M.; Wu, W.-C.; Mishra, S. R.; Tracy, J. B. Large-Scale Synthesis of Gold Nanorods through Continuous Secondary Growth. *Chem. Mater.* **2013**, *25*, 4537−4544.
(22) Vigderman, L.; Zubarev, E. R. High-Yield Synthesis of Gold Nanorods with Longitudinal SPR Peak Greater than 1200 nm Using Hydroquinone as a Reducing Agent. *Chem. Mater.* **2013**, *25*, 1450−1457.
(23) Lohse, S. E.; Eller, J. R.; Sivapalan, S. T.; Plews, M. R.; Murphy, C. J. A Simple Millifluidic Benchtop Reactor System for the High-Throughput Synthesis and Functionalization of Gold Nanoparticles with Different Sizes and Shapes. *ACS Nano* **2013**, *7*, 4135−4150.
(24) Isomaa, B.; Reuter, J.; Djupsund, B. M. The Subacute and Chronic Toxicity of Cetyltrimethylammonium Bromide (CTAB), a Cationic Surfactant, in the Rat. *Arch. Toxicol.* **1976**, *35*, 91−96.
(25) Park, K.; Drummy, L. F.; Wadams, R. C.; Koerner, H.; Nepal, D.; Fabris, L.; Vaia, R. A. Growth Mechanism of Gold Nanorods. *Chem. Mater.* **2013**, *25*, 555−563.
(26) Park, K.; Hsiao, M.-S.; Koerner, H.; Jawaid, A.; Che, J.; Vaia, R. A. Optimizing Seed Aging for Single Crystal Gold Nanorod Growth: The Critical Role of Gold Nanocluster Crystal Structure. *J. Phys. Chem. C* **2016**, *120*, 28235−28245.
(27) Watt, J.; Hance, B. G.; Anderson, R. S.; Huber, D. L. Effect of Seed Age on Gold Nanorod Formation: A Microfluidic, Real-Time Investigation. *Chem. Mater.* **2015**, *27*, 6442−6449.
(28) Walsh, M. J.; Barrow, S. J.; Tong, W.; Funston, A. M.; Etheridge, J. Symmetry Breaking and Silver in Gold Nanorod Growth. *ACS Nano* **2015**, *9*, 715−724.
(29) Park, K.; Hsiao, M.-S.; Koerner, H.; Jawaid, A.; Che, J.; Vaia, R. A. Optimizing Seed Aging for Single Crystal Gold Nanorod Growth: The Critical Role of Gold Nanocluster Crystal Structure. *J. Phys. Chem. C* **2016**, *120*, 28235−28245.
(30) Olea, A. F.; Thomas, J. K. Rate Constants for Reactions in Viscous Media: Correlation between the Viscosity of the Solvent and the Rate Constant of the Diffusion-Controlled Reactions. *J. Am. Chem. Soc.* **1988**, *110*, 4494−4502.
(31) Scarabelli, L.; Sánchez-Iglesias, A.; Pérez-Juste, J.; Liz-Marzán, L. M. A. Tips and Tricks" Practical Guide to the Synthesis of Gold Nanorods. *J. Phys. Chem. Lett.* **2015**, *6*, 4270−4279.
(32) Watt, J.; Hance, B. G.; Anderson, R. S.; Huber, D. L. Effect of Seed Age on Gold Nanorod Formation: A Microfluidic, Real-Time Investigation. *Chem. Mater.* **2015**, *27*, 6442−6449.
(33) Miller, O. D.; Polimeridis, A. G.; Reid, M. T. H.; Hsu, C. W.; DeLacy, B. G.; Joannopoulos, J. D.; Soljacic, M.; Johnson, S. G. Fundamental Limits to Optical Response in Absorptive Systems. *Opt. Express* **2016**, *24*, 3329−3364.
(34) Jia, H. L.; Fang, C. H.; Zhu, X. M.; Ruan, Q. F.; Wang, Y. X. J.; Wang, J. F. Synthesis of Absorption-Dominant Small Gold Nanorods and Their Plasmonic Properties. *Langmuir* **2015**, *31*, 7418−7426.
(35) Edgar, J. A.; McDonagh, A. M.; Cortie, M. B. Formation of Gold Nanorods by a Stochastic Popcorn Mechanism. *ACS Nano* **2012**, *6*, 1116−1125.
(36) Park, H. J.; Ah, C. S.; Kim, W. J.; Choi, I. S.; Lee, K. P.; Yun, W. S. Temperature-Induced Control of Aspect Ratio of Gold Nanorods. *J. Vac. Sci. Technol., A* **2006**, *24*, 1323−1326.
(37) Cheng, J.; Ge, L.; Xiong, B.; He, Y. Investigation of pH Effect on Gold Nanorod Synthesis. *J. Chin. Chem. Soc.* **2011**, *58*, 822−827.

DOI: 10.1021/acsami.7b08003
ACS Appl. Mater. Interfaces 2017, 9, 26363−26371